Environmentally friendly protective coatings for brake disks

A. Wank, C. Schmengler, A. Krause, K. Müller-Roden, T. Wessler, Luckenbach, GTV Verschleiss-Schutz GmbH, Luckenbach / D

Recently, environmental concerns have initiated intensive research and development in the field of friction brake systems with the aim to minimize particle emission. First brake systems that include thermally sprayed protective coatings on grey cast iron brake disks have been introduced in automotive industries and have proven suitability to strongly reduce particle emission. However, there is desire to use materials that show better environmental compatibility and lower price and to use processes that permit improved characteristics of protective coatings at reduced production costs. Different approaches concerning choice of base and coating materials as well as production processes are discussed with respect to technological, economic and ecological aspects. Besides grey cast iron also aluminum alloys are considered as base materials. For coating production HVOF spraying and laser cladding offer specific advantages and recent progress concerning the expansion of their production rate limitations is presented. Finally, novel feedstock materials that show excellent compatibility with stainless steel or aluminum alloy matrices have been developed and applied for coating production.

1 Introduction

There is a multitude of reasons for coating of automotive brake disks that are typically made of grey cast iron due to its excellent castability, machinability, high compressive strength and damping capacity, low notch sensitivity and low cost. Improvement of wear resistance could contribute to sustainability by prolonged lifetime and to environmental friendliness by reduced brake dust emission if adequate coating materials will be applied and brake pads will be adjusted to the coatings. Improvement of corrosion resistance is even a key factor for electric vehicles that use mostly regenerative braking but still require friction brakes for emergency braking events. Grey cast iron disks that form thick rust surface layers during long times of idleness will not permit adequate performance in such situations. But in the end esthetic features were the major reason for development and market introduction of coated grey cast iron brake disks. Hardmetal coatings on Porsche Surface Coated Brake (PSCB) disks do not form rust and result in up to 90% reduced brake dust emission in combination with their special brake pads. Therefore, both brake disk friction rings and aluminum wheels remain shiny metallic. In the meantime health and environmental concerns requiring reduction of brake dust emission that can contribute more than 50% to non-exhaust [1] and 20% to overall traffic related PM_{10} emissions [2] have become a major driving force for development of brake disk coating solutions.

Generally, different surface layer treatment and coating technologies are applicable for wear and corrosion protection of grey cast iron brake disks. Gaseous ferritic nitrocarburizing (FNC) can form roughly 20 µm thick surface layers that provide limited wear and corrosion protective function. Such coatings are predominantly useful to avoid rust formation on brake disk surfaces of new cars and thereby to maintain an appealing appearance prior to sales. Mass production would require use of large batch furnaces that will process thousands of disks simultaneously within two to four hours production time [3].

Thin film deposition techniques like PVD have been considered for coating of stainless steel scooter brake disks with roughly 5 µm thick TiAlN coatings to improve wear and thermal resistance. However, in abrasive wear tests that do not reflect tribological conditions of brake disks in an optimal way coatings were worn completely, and no significant improvement compared to uncoated AISI 410 steel was measured [4]. Graphite phase in grey cast iron that is more relevant for car brake disks makes deposition of PVD TiN or TiAlN coatings complicated due to formation of local bonding defects close to interfaces with graphite [5]. Pre-treatment with high energy beams like electron beams permits modification of grey cast iron surfaces that is suitable to avoid formation of such defects [6]. However, high investment costs and long production times of PVD coatings would result in very high costs of accordingly coated brake disks.

Graphite present at grey cast iron surfaces also complicates electroplating and even electroless plating. In early stages electroless nickel will not be deposited on graphite phase, although after longer processing time homogeneous plating thickness will be achieved. The strength of electroless platings on grey cast iron decreases strongly with graphite content. So, relatively weak bonding to graphite can be regarded as a type of defect [7]. Nevertheless, electroless nickel platings with only 10 µm thickness provide good corrosion protective function [8] and are already successfully used as corrosion protective layers on commercially available coated car brake disks. Generally, also hard chrome platings that have widely been used for combined wear and corrosion protection of workpiece surfaces can be deposited on grey cast iron. But electroplating processes involving carcinogenic hexavalent chromium are replaced more and more due to health concerns and the brittle coatings show a high density of microcracks [9] that could easily propagate under cycling thermo-mechanical load and in the end cause detachment of coating pieces. Just like thermochemical treatment and PVD processes electroplating and electroless plating processes require relatively long production time and are typically realized as batch processes, which makes integration into production lines complicated.

Contrary, thermal spray and built-up weld cladding processes permit coating deposition on individual workpieces at high deposition rates and in accordingly short time. Therefore, integration into production lines is quite easy and advantageous production costs can be reached.
Different approaches for production of protective coatings based on thermal spraying and laser cladding for grey cast iron and cast aluminum alloy brake disks will be presented and discussed concerning their effect on properties in use, costs, and impact on the environment.

2 Analysis of requirements for coating of automotive brake disk friction surfaces

The major function of a friction brake is to provide reliable conversion of kinetic energy into waste heat that needs to be dissipated into the environment. Brake rotor and pads form a tribological system and therefore optimal solutions could only be generated by holistic development of the pair. But these days typically pad materials that have been tailored to grey cast iron surfaces as counterparts for decades are used with or even without minor modifications for evaluation of brake disk coatings. So, brake disk coatings need to show a stable coefficient of friction when sliding against conventional and slightly modified brake pad materials in a wide range of interface temperatures, i.e., roughly from -40°C to 800°C [10,11].
Additionally, to permit long lifetime coatings must show high wear and oxidation resistance and high bond strength to base materials in a wide range of dynamic thermo-mechanical load. The coatings themselves must show high corrosion resistance, also against chlorides of de-icing salt, and must provide good corrosion protective function by preventing penetration of corrosive media to substrates with detrimental effect on bond strength. In contrast to laser claddings thermal spray coatings that are not fused or sealed cannot exclude presence or evolution of channels for local penetration by corrosive media. So, their use requires additional measures. Hardmetal coatings on Porsche Surface Coated Brake (PSCB) disks will even form a network of segmentation cracks during severe braking events. Electroless nickel platings as undercoats stop cracks and maintain the compound´s corrosion protective function. Generally, high temperature sealers could be applied on thermally sprayed coatings. But they would rather increase the tendency to form crack networks during severe braking events. Especially oxide ceramic coatings that show some strain tolerance due to presence of a microcrack network [12] will tend to form macrocracks after filling of microcracks. Corrosion protective laser claddings could be an alternative to nickel undercoats.
To improve environmental friendliness and health safety related to friction brake system dust emission, it is important not only to reduce PM_{10} emissions in general, but also to take care that the produced particles are not even more harmful than the currently emitted particles. As brake pads are required to become copper free, of course, brake disk coatings should not contain copper either. There is broad agreement that nickel and cobalt should not be released into the environment. Also, avoiding release of tungsten and its compounds is favored. Oxide ceramics based on alumina are considered particularly advantageous with respect to environmental friendliness, while chromia causes reservations, because formation of carcinogenic hexavalent chromium during coating production cannot be excluded. Also, titania particles with maximum size of 10 µm have been classified as potentially carcinogenic by the European Commission [13]. Zirconia based thermal spray coatings show smaller difference of thermal expansion behavior compared to the aforementioned oxide ceramics. But zirconia coatings show only low hardness, and their particularly low thermal conductivity hinders transfer of friction induced heat to the base material. Keeping in mind that automotive industry is particularly price sensitive, and materials need to be available in large quantities iron-based material solutions appear favorable. Besides martensitic stainless steels, iron based hard alloys with high contents of carbides or borides or iron based cermets appear to be promising candidates for production of environmentally friendly protective coatings for brake disks.
Depending on the applied coating process there are different limitations to be considered. In HVOF spraying processes heat transfer to particles can be tailored in a way that will permit softening of a metallic matrix component without initiating metallurgical reactions with hard phases that will strongly react with the matrix material, typically forming undesired brittle phases, e.g., in a sintering process. For example, even SiC based cermet coatings with nickel-based matrix can be produced successfully [14,15]. Also, high contents of hard phases can be applied without crack formation in respective coatings. Commercially available WC based cermet powders with FeCr or FeCrAl matrices that are advertised as environmentally friendly alternative to hardmetal with nickel or cobalt based matrices typically contain 85 wt.-%, which is about 75 vol.-%, WC. Slightly worse tribological performance of coatings with FeCrAl matrix compared to coatings with conventional cobalt-based matrix is attributed to formation of aluminum rich oxide inclusions during spraying [16]. As an alternative to WC TiC has been investigated as hard phase in iron-based matrix cermet coatings. Despite only 34 wt.-%, which is about 45 vol.-%, TiC in the composite powder comparable tribological performance like HVAF WC/CoCr coatings could be achieved [17]. Besides Cr_3C_2 that is frequently applied in combination with NiCr20 matrix for production of wear and corrosion protective HVOF coatings also NbC is considered as a promising hard phase for reinforcement of iron-based matrices. Recently, TiC/FeCr 70/30 (GTV 81.61.8), Cr_3C_2/FeCr 75/25 (GTV 80.82.1) and NbC/FeCr 80/20 (GTV 81.71.8) have been developed and tested for production of protective coatings on grey cast iron brake disks.
Among commercially available iron-based hard alloys FeCr(Ni)BSi materials permit achieving particularly high hardness of up to 850 HV0.3 upon average combined with excellent corrosion resistance. Therefore, such HVOF sprayed coatings have already been qualified for hard chromium replacement in printing industries [18]. Also, iron-

based alloys with high vanadium carbide content permit production of HVOF coatings with high hardness and corrosion resistance [19].
Production of laser claddings requires formation of a melt pool. So, there are much more intense metallurgical reactions compared to thermal spray processes. Also, contrary to HVOF spray processes that can generate coatings with compressive residual stress state, laser cladding is based on solidification and cooling of melt formed on a solid substrate, which results in tensile residual stress state. Therefore, it is not possible to produce crack free claddings with all materials that can be used to spray crack free coatings. Especially cladding of thin layers at high welding speed without substrate pre-heating results in particularly high crack probability. Studies on laser cladding at high welding speed have shown that crack formation cannot be avoided for use of FeCr(Ni)BSi alloy feedstock, while it is possible to clad iron-based alloys with high vanadium carbide content without crack formation, if preheating is carefully optimized along with tailoring of applied powder feed rate and laser power [20].
Limitations of achievable hard phase contents in cermet laser claddings do not only depend on heat management like pre-heating, but also the choice of material combination. While SiC and Cr_3C_2 dissolve rapidly in iron-based alloys and form brittle mixed carbides or oversaturated solid solution, TiC, VC and NbC fully re-precipitate after dissolution in iron-based melts without formation of brittle phases [21]. Therefore, significantly higher contents of TiC, VC and NbC can be realized in iron-based cermet laser claddings without crack formation. Fused tungsten carbide also forms brittle mixed carbides or oversaturated solid solution after dissolution in iron-based melts, but dissolution occurs significantly slower compared to SiC or Cr_3C_2.
Different TiC, VC and NbC powders have been combined with ferritic, duplex and austenitic stainless-steel powders to produce protective laser claddings on grey cast iron brake disks and to draw conclusions concerning optimal choice of powders and achievable cladding properties and productivity.
Applicability of laser-based surface technologies is also studied for manufacturing of wear protective layers on cast aluminum brake rotors. However, an adapted metallurgical approach is needed, because aluminum forms brittle intermetallic phases with most other elements. Also, most elements show lower affinity to carbon in comparison to aluminum, which results in formation of brittle needle shaped aluminum carbide precipitates, if carbides of such elements dissolve in an aluminum-based melt. As niobium shows stronger affinity to carbon compared to aluminum NbC laser dispersion tests are carried out.

3 Experimental

3.1 Thermal Spray Coatings

Thermal spray coatings have been produced using a liquid fuel HVOF spraying torch type GTV K2 and Exxsol D60 fuel. Applied spray parameters for different spray powders are listed in **table 1**. Chemical composition and particle size distributions of powders measured by laser scattering analyses using Quantachrome Cilas 920 equipment are listed in **table 2**.

Table 1. Applied spray parameters.

Powder	Cr_3C_2/FeCr 75/25 GTV 80.82.1	NbC/FeCr 80/20 GTV 81.71.8	FeCr25B5 GTV 80.44.1-0	FeCrV17 GTV 80.49.1
Nozzle	200/11	150K	150K	200/11
Oxygen [nlpm]	900	900	850	900
Fuel [l/h]	26	26	22	26
Powder feed rate [g/s]	2.17	1.67	1.67	2.17
Spray distance [mm]	350	350	350	350
Surface speed [m/s]	1.5	1.5	1.5	1.5
Track offset [mm]	5	5	5	5

Table 2. Chemical composition and particle size distribution of applied powders.

Powder	Cr_3C_2/FeCr 75/25 GTV 80.82.1	NbC/FeCr 80/20 GTV 81.71.8	FeCr25B5 GTV 80.44.1-0	FeCrV17 GTV 80.49.1
Fe [wt.-%]	20.1	15.3	Base	Base
Cr [wt.-%]	Base	5.2	24.3	12.6
C [wt.-%]	9.9	8.9	0.72	3.8
B [wt.-%]	-	-	5.12	-
Nb [wt.-%]	-	Base	-	-
V [wt.-%]	-	-	-	16.6
d_{10} [µm]	22.0	16.3	29.5	32.5
d_{50} [µm]	35.2	26.1	42.7	44.8
d_{90} [µm]	54.4	40.4	61.3	62.8

Coatings have been sprayed on roughly 250 µm thick stainless steel laser claddings that act as safe corrosion protective interim layers for friction ring areas of grey cast iron brake disks. The coatings are analyzed by optical microscopy and evaluated concerning porosity and bonding faults in the interface to the laser claddings. Additionally surface roughness and microhardness HV0.3 are analyzed.

3.2 Laser Claddings

Laser claddings have been produced using high power diode laser sources (Laserline GmbH, Mülheim-Kärlich, D) along with quasi-coaxial six-stream powder nozzles type GTV PN6625 (GTV Verschleiss-Schutz GmbH, D). Investigations started using a laser source LDF 6000-60 with a maximum beam power of 6.3 kW. To maximize productivity a LDF 16000-100 source with a maximum beam power of 16 kW and finally a LDF 22000-100 source with a maximum beam power of 22 kW have been applied. Applied process parameter ranges for different powder (mixtures) that permit deposition of layers with thickness between 80 - 600 µm are listed in **table 3**. Laser and powder foci coincide with the powder nozzle´s optimum working distance of 25 mm.

Table 3. Applied cladding parameter ranges.

Powder	stainless steel *	stainless steel *-NbC/FeCr 80/20 / TiC/FeCr 70/30	stainless steel *-NbC / TiC / VC **	stainless steel *-FTC spherical ***
Carbide powder content	-	< 40%	< 40%	< 50%
Laser power [kW]	2.8 - 22.0	3.0 - 22.0	3.0 - 22.0	13.0 - 22.0
Spot diameter [mm]	1.9 - 4.9	1.9 - 4.9	1.9 - 4.9	4.9
Welding speed [m/s]	0.67 - 6.7	0.67 - 6.7	0.67 - 6.7	2.5 - 6.7
Powder feed rate [g/s]	0.67 - 4.17	0.67 - 4.17	0.67 - 3.33	3.33 - 5.0
Overlap	60% - 95%	60% - 95%	60% - 95%	85% - 95%
Nozzle gas Ar [nlpm]	20 - 50	20 - 50	20 - 50	20 - 50
Carrier gas Ar [nlpm]	5 - 24	5 - 24	5 - 24	7 - 16

* AISI 430L (GTV 80.92.8), AISI 318LN (80.97.1), AISI 316L (GTV 80.46.1)

** Leached cubic NbC (CBMM, Brazil), sintered and crushed NbC (GTV 70.82.1), TiC (GTV 70.90.1), VC (GTV 70.80.1)

*** Spherical fused tungsten carbide (GTV 10.80.1S)

Dispersion of NbC/FeCr 80/20 into surfaces of cast aluminum disks is carried out using 11 kW laser power, 4.9 mm spot diameter, 25 nlpm Ar as nozzle gas, 1.27 g/s powder feed rate, 9.5 nlpm Ar carrier gas flow rate, 1.67 m/s welding speed and 92% overlap.
The coatings are analyzed by optical microscopy and evaluated concerning porosity and bonding faults in the interfaces between grey cast iron substrates and laser claddings and between individual laser cladding layers. Scanning electron microscopy and EDS analyses are carried out to evaluate dissolution and re-precipitation behavior of different hard phase particles. EBSD analyses are used to characterize crystallite size and shape and to analyze phase contents of stainless steel matrices. Additionally, microhardness HV0.3 measurements are carried out.

4 Results

4.1 Thermal Spray Coatings

HVOF spraying permits deposition of well adhering coatings with low porosity both for use of Cr_3C_2 or NbC based cermet powders with iron-based matrices and for use of iron-based hard alloy powders (**figure 1**). HVOF sprayed top coats cause a smoothening compared to corrosion protective laser claddings. Average roughness R_z is reduced from 70 - 80 µm to 25 - 35 µm for all produced coating compounds.
Cr_3C_2/FeCr 75/25 and NbC/FeCr 80/20 coatings show an average microhardness of 790 HV0.3 and 680 HV0.3 respectively, while average microhardness of 650 HV0.3 and 800 HV0.3 are determined for FeCrV17 and FeCr25B5 coatings respectively. There are only very few bonding defects between HVOF coatings and laser claddings, although there has been no machining of the laser claddings prior to HVOF spraying. All coating compounds can be ground to achieve adequate shape and position tolerances as well as a roughness R_z of less than 5 µm without crack formation.
In AMS braking tests on dynamometers iron-based hard alloy coatings tend to wear out with formation of grooves in circumferential direction by scratching without crack formation. Contrary, cermet coatings tend to form segmentation crack networks that are stopped at the interface between HVOF top coats and corrosion protective laser claddings. During prolonged testing horizontal cracks can form at the interface between laser claddings and HVOF coatings that will propagate and ultimately result in delamination of complete HVOF coating segments.

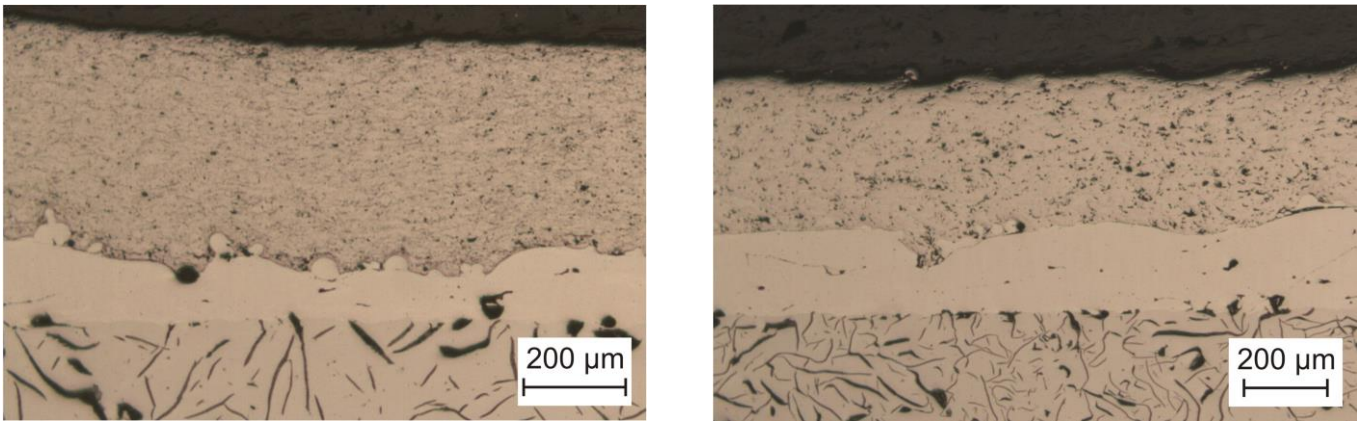

Figure 1. Optical micrographs of HVOF sprayed Cr_3C_2/FeCr 75/25 (left) and FeCr25B5 (right) coatings on AISI 318LN stainless steel laser claddings on grey cast iron brake disks.

4.2 Laser Claddings

Using a 1.9 mm spot diameter 2.8 kW laser power permits deposition of roughly 220 µm thick AISI 318LN claddings that provide secure corrosion protective function for grey cast iron substrates in two passes at welding speed of 0.67 m/s and 0.67 g/s powder feed rate (**figure 2**). There are only few imperfections in the interface between grey cast iron substrate and cladding and boundaries between the two laser cladding layers cannot be detected. Using the same set of process parameters also permits production of composite claddings consisting of AISI 318LN steel as matrix material and cubic NbC particles as reinforcing phase with graded content of NbC in the individual layers. NbC particles are fully embedded in the stainless steel matrix. Homogeneity of hard phase distribution is improved with increasing content and the number of imperfections in the interfaces between individual layers decreases with progressing cladding time (**figure 2**). Multi-layer compound claddings with graded content of hard phases are effective to avoid crack formation. In contrast to the 5-layer compound that can be produced without any cracks deposition of AISI 318LN / NbC 50/50 layers directly on a pure AISI 318LN layer results in cracking. Cladding of 0.1 m^2 friction ring surface area with the roughly 600 µm thick 5-layer compound consumes 17 minutes of active laser beam time. Including time for stabilizing of powder feed with the variable carbide contents total production time will be roughly 20 minutes.

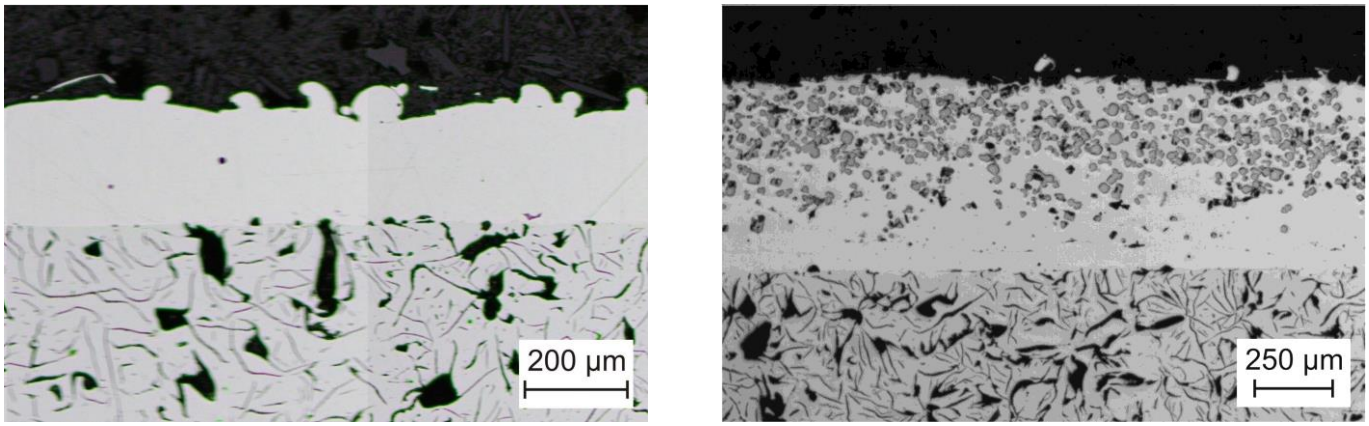

Figure 2. Optical micrographs of corrosion protective AISI 318LN cladding deposited in two passes (left) and 5-layer cladding consisting of AISI 318LN steel matrix and a graded content of 0%/10%/30%/50%/30% of cubic NbC particle reinforcement (right) on grey cast iron brake disks.

Use of cubic NbC particles shows advantages compared to use of irregular shaped fused tungsten carbide (W_2C/WC), Cr_3C_2 or SiC powder for reinforcement of stainless steel matrices, because its cubic shape permits very stable feeding and partial dissolution in stainless steel matrices does not result in formation of brittle phases and finally in crack formation. Contrary, dissolved niobium and carbon form submicron sized equiaxed precipitates during solidification and cooling of the cladding (**figure 3**). However, the production process of cubic NbC particles is based on leaching of an iron based matrix with some aluminum content, which results in alumina contamination of the NbC feedstock. During cladding alumina impurities cause a strong increase of emission in the process zone and result in formation of craters that can cover the complete thickness of a layer that is being deposited (**figure 3**). Use of either sintered and crushed NbC or agglomerated and sintered NbC/FeCr 80/20 powders both permits avoiding crater formation securely. While spherical agglomerated and sintered NbC/FeCr 80/20 powders permit high feed rate stability, irregular shaped NbC particles easily cause pulsing powder feed or even blocking of powder feed lines. Problems increase with increasing powder feed rate and reduced carrier gas flow rate, which is an

important parameter and must be optimized carefully as it strongly influences the speed of particles on their way into the melt pool and accordingly their dwell time and interaction with the laser beam.

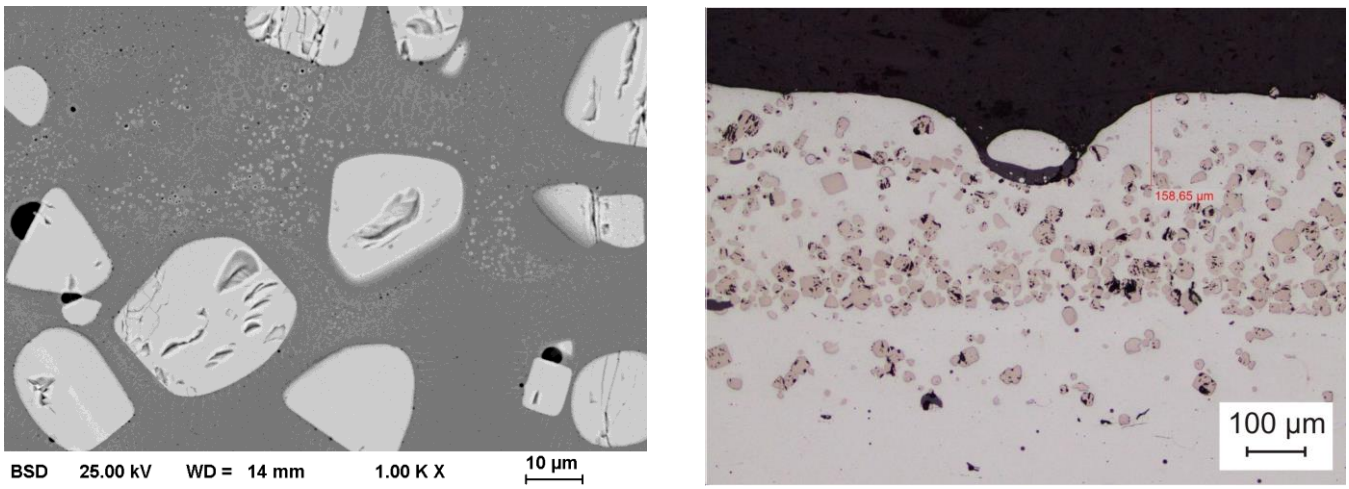

Figure 3. SEM micrograph of a cubic NbC reinforced AISI 318LN stainless steel laser cladding (left) and optical micrograph of alumina impurity induced crater formation in a 4-layer cladding consisting of AISI 318LN stainless steel matrix and cubic NbC reinforcement (right).

Sintered and crushed powders show relatively large specific surface areas. Therefore, there is stronger dissolution in the melt pool compared to cubic NbC and agglomerated and sintered NbC/FeCr composite particles. Besides submicron sized equiaxed precipitates there are also dendritic NbC precipitates in areas, where the stainless steel melt pool became strongly enriched by niobium and carbon (**figure 4**). Sintered and crushed NbC particles keep their microstructure that is characterized by imperfect interfaces of primary particles that got sintered and by cracks that evolved during the crushing process and did not result in complete break-up of individual particles. If stainless steel matrix melt does not penetrate such cracks, these cracks become part of the overall microstructure of the claddings and represent nuclei for crack propagation under dynamic thermo-mechanical load during braking events.

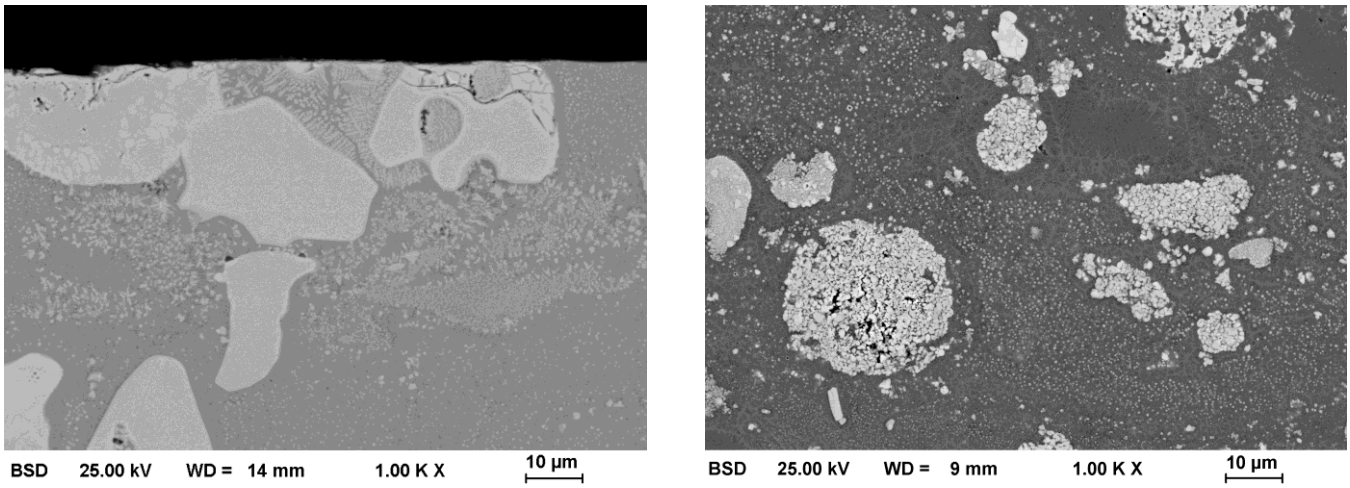

Figure 4. SEM micrographs of AISI 318LN stainless steel laser claddings with sintered and crushed NbC reinforcement (left) and with agglomerated and sintered NbC/FeCr 80/20 reinforcement (right).

Agglomerated and sintered NbC/FeCr 80/20 particles are mostly spherical and therefore show low surface area. Accordingly, limited dissolution of niobium and carbon in stainless steel melt results in formation of submicron sized equiaxed precipitates during solidification and cooling of the cladding (**figure 4**). The microstructure of such composite coatings also contains relatively small composite particles that got melted due to interaction with the laser beam on their way into the melt pool. These particles are embedded in the stainless steel matrix that is reinforced by submicron equiaxed NbC precipitates and show full density and carbide size even smaller than the primary carbides that are used for production of the powder feedstock. Finally, the composite coatings contain relatively big composite particles that retain the original porous microstructure of agglomerated and sintered NbC/FeCr 80/20 feedstock particles. These particles represent the weakest component of the composite claddings due to their limited cohesive properties. During metallographic preparation of cross section some local breakout can occur leaving micro-craters. The same can happen during grinding of the protective coatings to achieve adequate smoothness as

well as required position and shape tolerances. Such microcraters are typically filled with brake pad material very fast during braking events.
Crack free claddings can be produced securely without pre-heating using up to 40 wt.-% niobium carbide feedstock. During grinding of such claddings crack formation can be avoided securely, too. EDS analyses that cannot take carbon content into consideration show basically the same mass content of niobium in composite claddings like the content of NbC in the applied powder mixtures. Claddings produced with 30 wt.-% NbC/FeCr 80/20 only show crack formation after multiple extreme braking events.
In a cladding test series using mixtures of AISI 316L stainless steel as matrix material and sintered and crushed carbides that are known not to form brittle mixed phases, i.e., NbC (GTV 70.82.1), VC (GTV 70.80.1) and TiC (GTV 70.80.1), for reinforcement likeliness of crack formation depending on carbide type has been studied. NbC permits avoiding crack formation up to a carbide content of 40 wt.-%, which is about 40 vol.-%, without necessity of pre-heating. Contrary, for use of TiC a maximum carbide content of 20 wt.-%, which is about 29 vol.-%, could be realized without crack formation and for use of VC even a carbide content of only 15 wt.-%, which is about 20 vol.-%, did not permit avoiding crack formation without pre-heating. Although these three carbides fully re-precipitate as monocarbides without formation of brittle mixed phases and their thermal expansion behavior is very similar (NbC $6{,}7 \cdot 10^{-6}$ K^{-1}, VC $7{,}2 \cdot 10^{-6}$ K^{-1}, TiC $7{,}7 \cdot 10^{-6}$ K^{-1} [22]) crack formation tendency differs significantly.
With the aim to improve productivity cladding tests at up to 22 kW laser power have been conducted. Thereby two-layer compounds consisting of AISI 318LN or AISI 430L stainless steel base layers and top layers with the same steel matrix reinforced by 30 wt.-% NbC/FeCr 80/20 have been produced (**figure 5**). Production of compounds with 150 µm and 300 µm average thickness of base and top layer respectively on 0.1 m^2 friction ring surface area only takes 154 s active laser time. Including time for stabilizing of powder feed total production time will be about 180 s, which is by factor 6.7 faster compared to production time for 6 kW laser power. Consumption of steel and carbide powder will be roughly 375 g and 100 g respectively. The claddings show low porosity and only very few oxide inclusions and imperfections in the interfaces both between grey cast iron substrate and claddings and between the two cladding layers. There is a homogeneous distribution of carbides in the top layer with about 30 vol.-% carbide content according to digital image analyses for both types of matrix materials. But average microhardness of claddings with AISI 430L matrix is significantly higher compared to AISI 318LN matrix (660 HV0.3 vs. 500 HV0.3), while AISI 430L layers without carbide reinforcement are softer than AISI 318LN claddings (220 HV0.3 vs. 270 HV0.3).

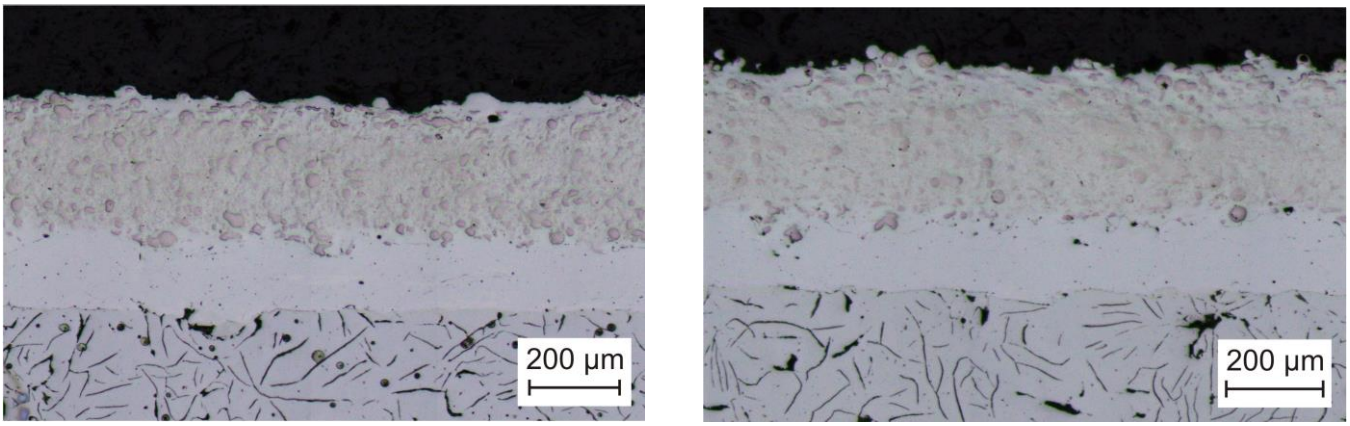

Figure 5. Optical micrographs of double layer claddings with AISI 318LN (left) and AISI 430L (right) stainless steel matrices and 30 wt.-% reinforcement by agglomerated and sintered NbC/FeCr 80/20 powder in the top layer, produced at 22 kW laser power

As TiC is significantly cheaper than NbC not only NbC/FeCr 80/20, but also TiC/FeCr 70/30 feedstock has been developed to try and exploit the advantageous feed rate stability that is offered by spherical agglomerated and sintered powders also for TiC based feedstock and to investigate its applicability as an alternative to NbC/FeCr 80/20. Crack free two-layer compounds consisting of AISI 318LN or AISI 430L stainless steel base layers and top layers with the same steel matrix reinforced by 24 wt.-% TiC/FeCr 70/30 have been produced (**figure 6**). However, crack formation in AISI 318LN - 24 wt.-% TiC/FeCr 70/30 claddings could only be avoided by pre-heating to 200°C. Identical production time compared to use of 30 wt.-% NbC/FeCr 80/20 reinforcement has been achieved. Consumption of steel and carbide powder is roughly 380 g and 75 g respectively.
The claddings show low porosity and only very few oxide inclusions and imperfections in the interfaces both between grey cast iron substrate and claddings and between the two cladding layers. Due to the lower density of TiC in comparison to NbC also about 30 vol.-% carbide content is determined in digital image analyses. Like in claddings produced with NbC/FeCr feedstock for reinforcement average microhardness of claddings with AISI 430L matrix is significantly higher compared to those with AISI 318LN matrix (640 HV0.3 vs. 470 HV0.3), while AISI 430L layers without carbide reinforcement are softer than AISI 318LN claddings (220 HV0.3 vs. 260 HV0.3).
Carbides are homogeneously distributed in the top layer, but there is multiple break-out of coarse TiC/FeCr composite particles during metallographic preparation. The effect occurs preferentially close to the interface between the two cladding layers and close to the surface, i.e., in places, where the melt pool solidifies particularly fast and met-

allurgical interaction between stainless steel melt and composite particles is accordingly poor. A weaker cohesive strength within individual composite powder particles of TiC/FeCr compared to NbC/FeCr can be concluded. Claddings on brake disks need to be ground to achieve an adequately smooth surface and to meet requirements concerning position and shape tolerances. Such grinding procedure is typically less gentle than metallographic preparation and formation of microcraters is very likely.

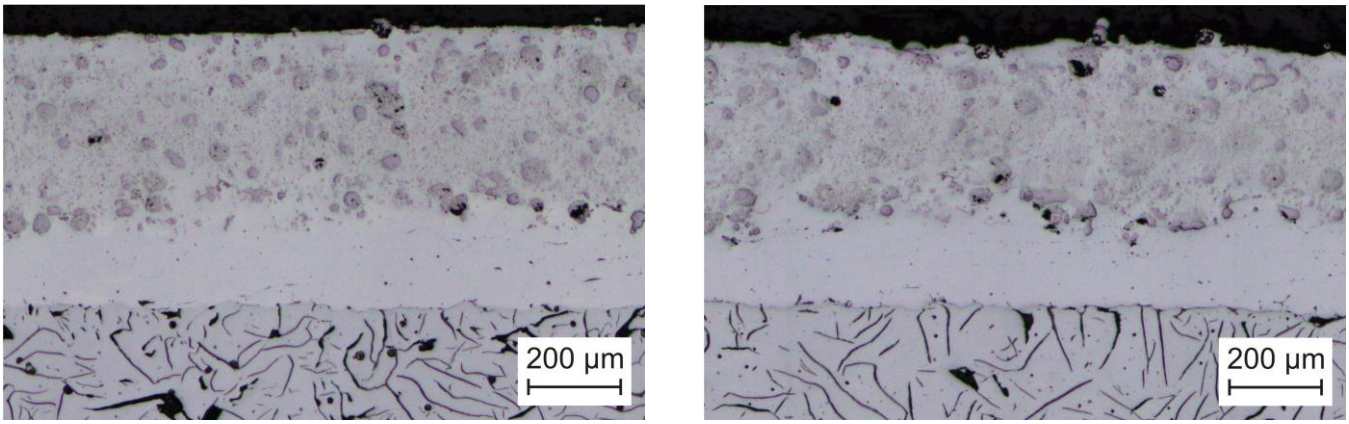

Figure 6. Optical micrographs of double layer claddings with AISI 318LN (left) and AISI 430L (right) stainless steel matrices and 24 wt.-% reinforcement by agglomerated and sintered TiC/FeCr 70/30 powder in the top layer, produced at 22 kW laser power

As claddings are produced with strong overlap of typically 90 - 95%, individual layers are formed by stacking of multiple seams. Depending on applied cladding parameters surfaces of previously deposited seams will be remelted completely or partially during deposition of subsequent seams (**figure 7**). Concurrent with heat flux there is directional solidification. In locations, where seam surfaces are remelted, crystallites can grow epitaxially and cover the total 100 - 150 µm layer thickness. EBSD analyses of AISI 318LN claddings show an only negligible austenite content. While other studies that covered much lower welding speed in the range of several mm/s report about 5% austenite phase [23] in AISI 318LN claddings, only 0.3% have been detected in claddings that are produced at a welding speed of 3.3 m/s.

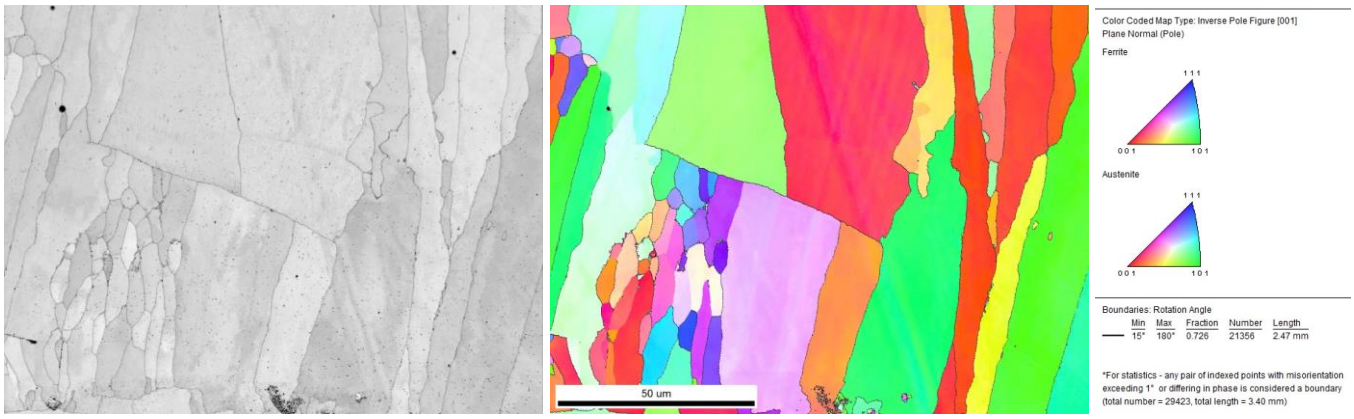

Figure 7. EBSD analysis of an AISI 318LN cladding deposited on a grey cast iron brake disk showing local epitaxial growth of directionally solidified crystals with length covering the thickness of multiple stacked seams forming the layer and local division between crystallites at a seam surface that was not remelted during the cladding process

After careful tailoring of heat transfer to stainless steel and fused tungsten carbide powder particles on their way through the laser beam into the formed melt pool and to stainless steel buffer layers on grey cast iron brake disks in combination with suitable pre-heating, it is possible to produce crack free claddings that can reach a content of 33 vol.-% fused tungsten carbide (**figure 8**). Cladding conditions must be chosen adequately to avoid dissolution of tungsten carbide in the steel matrix and tensile stresses in the cladding due to shrinkage must be limited. Production of compounds with 120 µm and 280 µm average thickness of base and top layer respectively on 0.1 m^2 friction ring surface area only takes 110 s active laser time. Including time for stabilizing of powder feed total production time will be about 135 s.

In contrast to cladding layers with reinforcement by NbC/FeCr or TiC/FeCr microhardness testing results in extreme scattering of individual values ranging from 400 - 2,500 HV0.3 with 400 HV0.3 representing areas with maximum distance to surrounding carbide particles and 2,500 HV0.3 representing tests in the center of carbide particles. Average microhardness values of ten measurements are in the range between 900 HV0.3 and 1,400 HV0.3. Due to the extremely large standard deviation of measured values average microhardness is not meaningful.

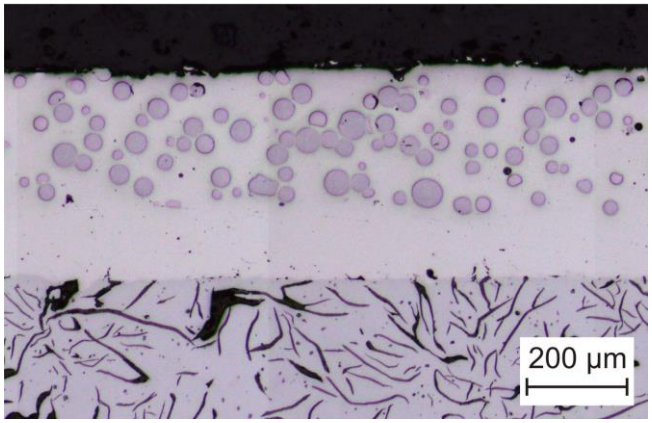

Figure 8. Optical micrograph of a double layer cladding with AISI 316L stainless steel matrix and 45 wt.-% reinforcement by spherical fused tungsten carbide powder in the top layer, produced at 20 kW laser power and after pre-heating to 300 °C

Stainless steel claddings reinforced by spherical fused tungsten carbide show lower waviness, i.e., smaller scattering of local cladding thickness values, than NbC/FeCr or TiC/FeCr reinforced claddings. That could be advantageous concerning grinding to achieve the required smooth surface and position and shape tolerances. However, besides local thickness deviations also distortion of brake disks needs to be considered to quantify required machining tolerances and resulting grinding efforts. Distortion of brake disks after laser cladding processes is complex. Besides distortion in radial direction also distortion in circumferential direction of the friction ring as well as distortion between flange and friction ring plane need to be considered. Distortion strongly depends on the design of brake disks and on the residual stress state of pre-machined brake disks prior to cladding. At least for some brake disk design disks from different casting and pre-machining batches that are clad in random sequence will show position and shape tolerances clearly correlating with their batch. In such case stress relief annealing prior to pre-machining might save a lot of costs for production of thick claddings that need to be ground much.
Distortion increases with heat transfer to brake disks during the cladding process. Use of higher laser power and short production time results in reduced overall heat transfer and accordingly lower distortion. Distortion, of course, also increases with thickness of deposited claddings. Depending on brake disk design there can be more than 1 mm radial distortion after cladding of one side with a carbide reinforced stainless steel composite cladding that shows 600 - 700 µm thickness. Subsequent cladding of the other side typically does not result in full recovery of the initial shape. Tailoring of welding strategy during cladding of brake disks with multiple layers is a key factor to minimize final distortion and accordingly minimize costs for cladding production and grinding process.
Stainless steel claddings with 30 vol.-% NbC/FeCr reinforcement in the top layer show excellent performance in AMS braking tests on dynamometers. Crack formation can be avoided securely if adapted brake pad materials will be applied. Only prolonged crack initiation tests will finally result in formation of vertical cracks. High temperatures of more than 800°C evolving during such braking events result in oxidation of carbides that are exposed to the atmosphere on crack surfaces (**figure 9**). Carbides that remain fully embedded in the stainless steel matrix do not oxidize.

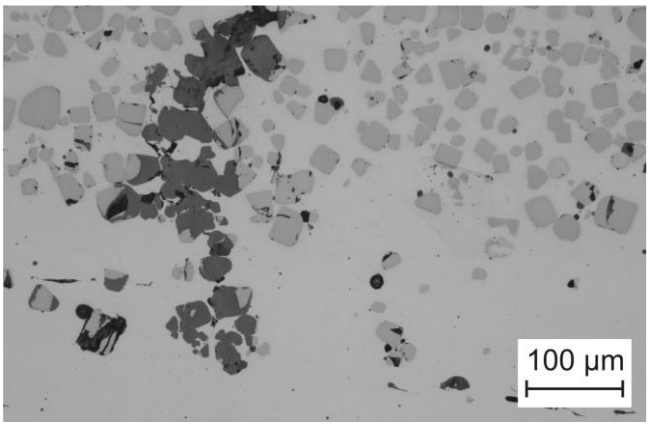

Figure 9. Optical micrograph showing oxidized NbC particles on the surfaces of cracks that evolve during prolonged crack initiation tests.

Reinforcement of cast aluminum alloy brake disks by laser dispersing of NbC/FeCr 80/20 is successfully achieved. Use of powder mixtures of NbC/FeCr 80/20 - 50 wt.-% AlSi12Cu12 permits limiting the content of NbC in the reinforced surface layers to a maximum of 60 vol.-% and to achieve a very homogeneous distribution of NbC simultaneously (**figure 10**). Such surface layers show an average microhardness of 550 HV0.3. Depending on surface speed and powder feed rate surface layers with 200 - 500 µm thickness have been realized. Manufacturing of

500 µm thick surface layers with 60 vol.-% NbC reinforcement on 0.1 m^2 friction ring surface area takes 150 s active laser time, which is almost equal to the overall production time, because no change of powder composition is needed.

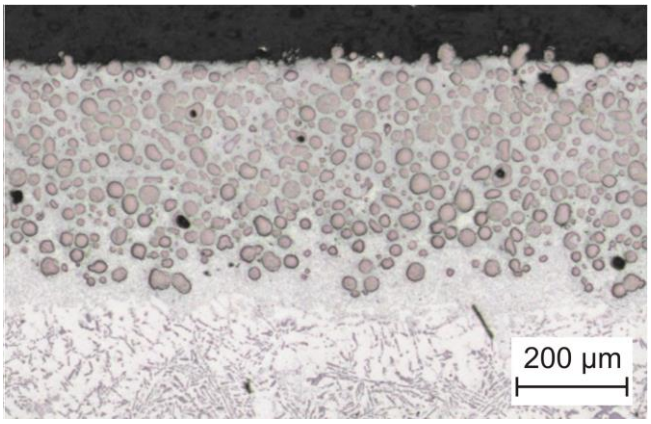

Figure 10. Optical micrograph of a low-pressure die cast hypereutectic Al-Si alloy brake disk reinforced with a mixture of AlSi12Cu12 - 50 wt.-% NbC/FeCr 80/20 by laser dispersion process.

Surface layers with carbide content exceeding 30 vol.-% could only be deposited without crack formation if brake disks were pre-heated prior to laser surface treatment. Laser surface remelting prior to laser dispersion is an effective method to avoid considerable porosity levels.

5 Discussion

Generally, both thermal spray and laser cladding technologies prove to be suitable technologies for production of protective coatings for automotive brake disks. Thermal spraying permits production of smoother coatings and to realize significantly higher hard phase contents in coatings without crack formation. However, there is no metallurgical bonding to substrates and thermally sprayed coatings alone cannot exclude penetration by corrosive media with subsequent failure due to corrosion of the substrate in the interface zone. Contrary, laser claddings can exclude penetration by corrosive media securely. So, they can be used as corrosion protective buffer layers between grey cast iron substrates and thermally sprayed top coats. There is a variety of iron based hard alloys and cermets with iron-based matrices that can be sprayed to achieve wear protective top coats that will not release nickel, cobalt and copper into the environment due to wear. While iron based hard alloys seem to show rather limited wear resistance in combination with several brake pad materials, cermets show high wear resistance due to their high content of hard phases. However, they tend to from a segmentation crack network during severe braking events, which can finally result in chipping of coating fragments.
Crack free laser claddings cannot be produced with the high contents that can be realized in thermally sprayed coatings. It is possible to produce crack free wear protective claddings with stainless steel matrix and carbide contents of roughly 30 vol.-% for use of NbC, TiC and spherical fused tungsten carbide as reinforcing phases. Among the three carbides NbC permits avoiding crack formation in the most robust way. While 30 vol.-% TiC can only be achieved for use of some stainless steel matrices without pre-heating, 30 vol.-% fused tungsten carbide reinforcement additionally requires very careful tailoring of heat transfer to powder particles and substrate surface to basically exclude dissolution of fused tungsten carbide in the steel melt. Despite those challenges for cladding process control and concerns with respect to release of tungsten into the environment, spherical fused tungsten carbide still appears to be an attractive hard phase, because it is readily available as a proven powder product from various suppliers, and it permits production of particularly smooth claddings.
TiC is a particularly cost advantageous hard phase and the raw material price cannot be influenced strongly by individual countries, while tungsten and niobium raw material price evolution is dominated by China and Brazil respectively. However, there is more need to improve quality of powder feedstock compared to NbC and formation of TiO_2 during severe braking might result in brake dust emission that is classified as potentially carcinogenic.
Stainless steels that solidify mostly with ferritic crystal structure show lower crack formation tendency compared to austenitic stainless steels, which can be attributed to their lower thermal expansion coefficient. However, AISI 430L steel shows relatively poor resistance to local corrosion induced by chlorides. Duplex steels like AISI 318LN solidify almost only with ferritic crystal structure at high welding speed and show excellent resistance to chlorides.
Laser cladding permits fulfilling demands concerning corrosion and wear protective function of friction ring coatings with a single coating process and features metallurgical bonding to the substrate and between individual layers. Use of high-power laser sources permits fast production. Disks showing 0.1 m^2 friction ring surface area can be clad within less than 3 minutes.
Generally, there are several solutions for environmentally friendly corrosion and wear protective coatings for automotive brake disks readily available. But detailed investigations on the effect of wear debris on creatures is still

needed. Besides overall emission of PM_{10} particles during wear of brake disks and pads also the health impact of specific debris needs to be analyzed. For that it is vitally important to develop specifically adjusted brake pads that will show significantly reduced wear compared to state-of-the-art brake pads and that will simultaneously avoid detrimental effect on corrosion protective properties of the newly developed coatings. Especially transfer of mild steel wool onto the surfaces of brake disks could initiate local corrosion by damage of the passivation layer that protects stainless steel matrices.
Recently developed monitoring and control tools for laser cladding processes permit a new level of reproducibility and process stability. Among these tools are closed-loop weight-loss controlled powder feeders, melt pool monitoring by pyrometry or thermography, offline and online digital image analyses of powder jets exiting powder nozzles and monitoring of optics by scattered light sensors and calorimeters integrated into laser cladding systems [24]. Holistic research that covers the complete production chain of coated brake disks is needed to achieve optimal productivity. Coatings need to be considered already in the stage of brake disk design. Tribological performance of substrate materials does not have to be considered anymore. So, grey cast iron materials that contain less graphite and result in less challenging surface states for cladding processes could be chosen. Connection between brake disk flange and friction ring needs to be designed adequately to achieve minimal sensitivity to coating process related heat transfer resulting in distortion. Suitable welding strategies that contribute to minimal distortion of clad brake disks need to be developed. Finally, coatings need to be developed along with grinding processes. Grinding behavior differs strongly depending on coating material. Small cost savings due to choice of a cheaper feedstock material in coating processes might result in strongly increased grinding costs.

6 Summary and Conclusions

A variety of environmentally friendly coating solutions for protection of automotive grey cast iron brake disks has been developed successfully. Besides multi-layer laser cladding solutions also combinations of corrosion protective laser cladding buffer layers and thermally sprayed top coats show general aptitude. For cast aluminum alloy brake rotors laser dispersion of NbC has been identified as a promising approach. Use of high power lasers permits achieving cycle times that are relevant for mass production. However, there is need to develop adjusted brake pads to exploit the full potential of the developed coating solutions and coatings need to be considered already in the design phase of novel brake disks to permit achieving optimal productivity and product performance. Finally, joint development of coating materials and grinding processes is crucial to minimize overall production costs.

Literature

[1] Harrison, R.M., A.M. Jones, J. Gietl, J.X. Yin, D.C. Green: Estimation of the contributions of brake dust, tire wear, and resuspension to nonexhaust traffic particles derived from atmospheric measurements. Environmental Science and Technology, Vol. 46 (2012) 12, pp. 6523-6529.
[2] Grigoratos, T., G. Martini: Brake wear particle emissions: a review. Environmental Science and Pollution Research, Vol. 22 (2015), pp. 2491-2504.
[3] Titus, J.: FNC and gas nitriding use in applications where reduced surface friction is a requirement. Gearsolutions, June 2014, p. 24.
[4] Kumar, M.S., S. Vishal, V. Visisht: Improvement in Wear and Thermal Resistance of Disc Brake Rotors using TiAlN Coating. International Journal of Science and Research, Vol. (2017) 7, pp. 366-372.
[5] Hsu, C.H., J.K. Lu, K.L. Lai, M.L Chen: Erosion and Corrosion Behaviors of ADI Deposited TiN/TiAlN Coatings by Cathodic Arc Evaporation. Materials Transactions, Vol. 46 (2005) 6, pp. 1417-1424.
[6] Buchwalder, A., N. Klose, R. Zenker, M. Engelmann, M. Steudtner: Utilisation of PVD Hard Coating after Electron Beam Surface Treatment for Cast Iron. HTM Journal of Heat Treatment and Materials, Vol. 71 (2016) 6, pp. 258-264.
[7] Yamada, T., A. Yamamoto, M. Fujiwara, Y. Kunugi: Strength evaluation and effect of graphite on strength of electroless nickel plating on cast iron. Journal of Materials Science, Vol. 28 (1993) 13, pp. 3513-3518.
[8] Hsu, C.H., J.K. Lu, R.J. Tasi: Characteristics of duplex surface coatings on austempered ductile iron substrates. Surface and Coatings Technology, Vol. 200 (2006) 20-21, pp. 5725-5732.
[9] Krelling, A.P., M.M.D. Souza, C.E.D. Costa, J.C.G. Milan: HVOF-sprayed coating over AISI 4140 steel for hard chromium replacement. Materials research, Vol. 21 (2018) 4, pp. 3-12.
[10] Jacko, M.G.: Physical and Chemical Changes of Organic Disc Pads in Service. Wear, Vol. 46 (1978) 1, pp. 163-175.
[11] Demir, A., R. Samur, I. Kilicaslan: Investigation of the coatings applied onto brake discs on disc-brake pad pair. Metalurgija, Vol. 48 (2009) 3, pp. 161-166.
[12] Samur, R., A. Demir: Wear and corrosion performances of new friction materials for automotive industry. Metalurgija, Vol. 51 (2012) 1, pp. 94-96.
[13] Commission Delegated Regulation (EU) 2020/217 (14th Adaptation to Technical and Scientific Progress, ATP) amending Regulation (EC) No. 1272/2008 (CLP Regulation).
[14] Wielage, B., J. Wilden, T. Schnick, A. Wank: Development of SiC composite feedstock for HVOF applications. Proc. ITSC 2002, Essen, D, March 4th - 6th, 2002, pp. 749-754.

[15] Wielage, B., J. Wilden, T. Schnick, A. Wank, J. Beczkowiak, R. Schülein, H. Zoz, H. Ren: Mechanically alloyed SiC composite powders for HVOF applications. Proc. ITSC 2002, Essen, D, March 4th - 6th, 2002, pp. 1047-1051.
[16] Testa, V., S. Morellia, G. Bolelli, B. Benedetti, P. Puddu, P. Sassatelli, L. Lusvarghi: Alternative metallic matrices for WC-based HVOF coatings. Surface and Coatings Technology, Vol. 402 (2020), Article 126308.
[17] K. Bobzin, M. Öte, T.F. Linke, K.M. Malik: Wear and Corrosion Resistance of Fe-Based Coatings Reinforced by TiC Particles for Application in Hydraulic Systems. Journal of Thermal Spray Technology, Vol. 25 (2016) 1-2, pp. 365-374.
[18] Wank, A., A. Schwenk, X. Shen: Hard chromium replacement by HVOF sprayed iron based coatings in printing industries. Thermal Spraying Technology, Vol. 30 (2010) 3, pp. 55-60.
[19] Wielage, B., A. Wank, H. Pokmurska, U. Dilthey, B. Balashov, J. Gollnick, L. Stein, S. Kondapalli, E. Deppe, T. Schnick: HVOF sprayed high chromium and high vanadium containing iron based hard coatings for combined abrasive wear and corrosion protection. Proc. ITSC 2005, Basel, CH, May 2nd - 4th, 2005, pp. 887-891
[20] Schmengler, C., A. Hitzek, A. Wank: Capability of High Speed Laser Cladding Process with Iron-based Alloys. Proc. ITSC 2019, Yokohama, JP, May 26th - 29th, 2019, pp. 659-665.
[21] Hofer, B.: Heiß-Isostatisches-Pressen (HIP) Anwendungen in der Kunststoffmaschinenindustrie. Proc. SKZ Conference Verschleiß und Verschleißschutz an Kunststoffverarbeitungsmaschinen, slide 31.
[22] Bauccio, M.: ASM Engineered Materials Reference Book, 2nd edition, ASM International, Materials Park, OH, USA, 1994.
[23] Karl, A.: Laserauftragschweißen hochlegierter Duplexstähle. Werkstofftechnik Aktuell, Vol. 10, Eds.: P. Schaaf, E. Rädlein, Universitätsverlag Ilmenau, 2014.
[24] Wank, A., C. Schmengler, A. Hitzek, A. Krause, M. Mülln: Progress in Laser Additive Manufacturing Equipment and Applications. Journal of Japan Laser Processing Society, Vol. 29 (2022) 1, pp.1-6